

N90-21084

Experimental Evaluation of Active-Member Control of Precision Structures

James Fanson, Gary Blackwood, and Cheng-Chih Chu
Jet Propulsion Laboratory
California Institute of Technology
Pasadena, California

NASA/DOD CSI Conference
January 29-February 2, 1989

PRECEDING PAGE BLANK NOT FILMED

387

TECHNOLOGY OBJECTIVES

This paper describes the results of closed-loop experiments that use piezoelectric active-members to control the flexible motion of a precision truss structure. These experiments are directed toward the development of high-performance structural systems as part of the Control/Structure Interaction program at JPL. The focus of CSI activity at JPL is to develop the technology necessary to accurately control both the shape and vibration levels in the precision structures from which proposed large space-based observatories will be built. Structural error budgets for these types of structures will likely be in the sub-micron regime; optical tolerances will be even tighter. In order to achieve system level stability and local positioning at this level, it is generally expected that some form of active control will be required.

- **STATIC STRUCTURAL PERFORMANCE**

- Order-of-magnitude improvement in geometric shape control over passive structures (Micron Level)
- Active compensation for thermal gradient distortion

- **DYNAMIC STRUCTURAL PERFORMANCE**

- Order-of-magnitude improvement in dynamic stability over passive structures

- **ON-ORBIT ADAPTABILITY**

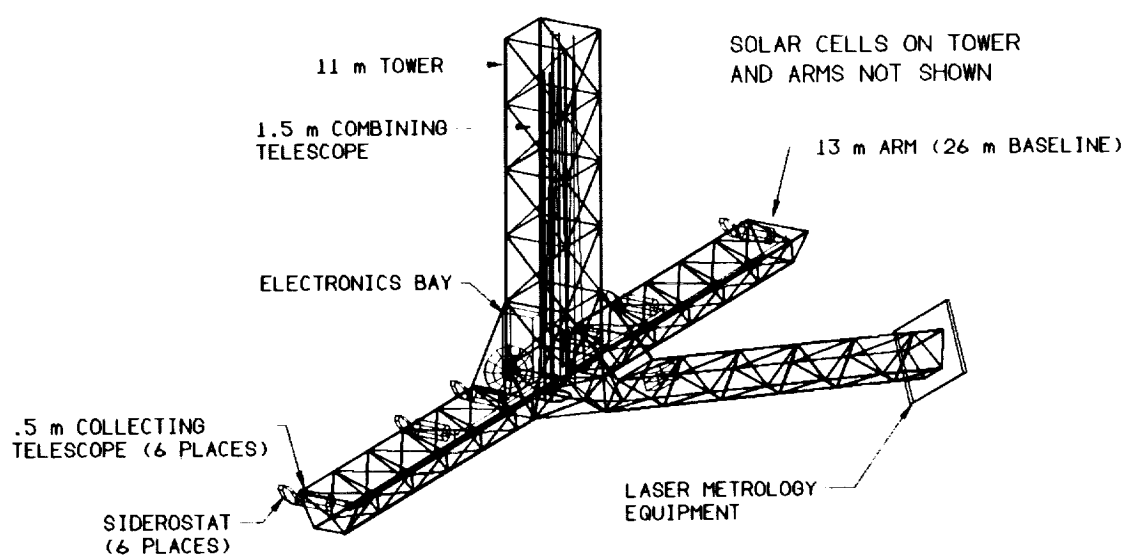
- Ease requirements on ground tests
- Enable a versatile structural *system* that can adapt its characteristics to meet changing mission requirements

- **SYSTEM IDENTIFICATION**

- Enable a means of on-orbit system identification and modal testing

JPL CSI FOCUS MISSION: INTERFEROMETER

One application of precision controlled structures, which has become the focus mission for the JPL CSI program, is an orbiting interferometer telescope¹. The interferometer works by precisely positioning small aperture telescopes separated by large baselines, thereby synthesizing a larger effective aperture and enabling greater imaging resolution. In order to function, the path lengths traversed by starlight striking the various component telescopes must be held constant to a small fraction of the wavelength of light being observed. For an ultraviolet interferometer, this corresponds to path length stability on the order of a few nanometers over distances of tens of meters of relatively lightweight and possibly flexible spacecraft structure.



FMI CONFIGURATION

ACTIVE STRUCTURES APPROACH

One approach to controlling the elastic deflections of truss structures is to use active-members--structural elements with actuators and sensors built into them. A control system can be designed around these active-members to provide "intelligent structure" performance beyond that achievable for conventional structures of comparable weight. Piezoelectric actuators are employed in the JPL active-member design. Previous experiments in active-member control include the use of voice-coil type actuators in one and two bay trusses at TRW and Caltech.^{2,3} PID* controllers have also been implemented on a similar structure in Japan.⁴ Early work on the use of piezoelectrics for structural control concentrated on the use of flat piezoelectric crystals to control the vibrations of uniform beams.^{5,6,7,8} More recent work at MIT has concentrated on the use of piezoelectrics embedded in structural truss members and passively shunted to introduce damping.⁹ Concurrent active-member research at JPL in support of the Precision Segmented Reflector program is reported elsewhere.¹⁰

*proportional integral differential

PIEZOELECTRIC ACTIVE-MEMBERS

ADVANTAGES

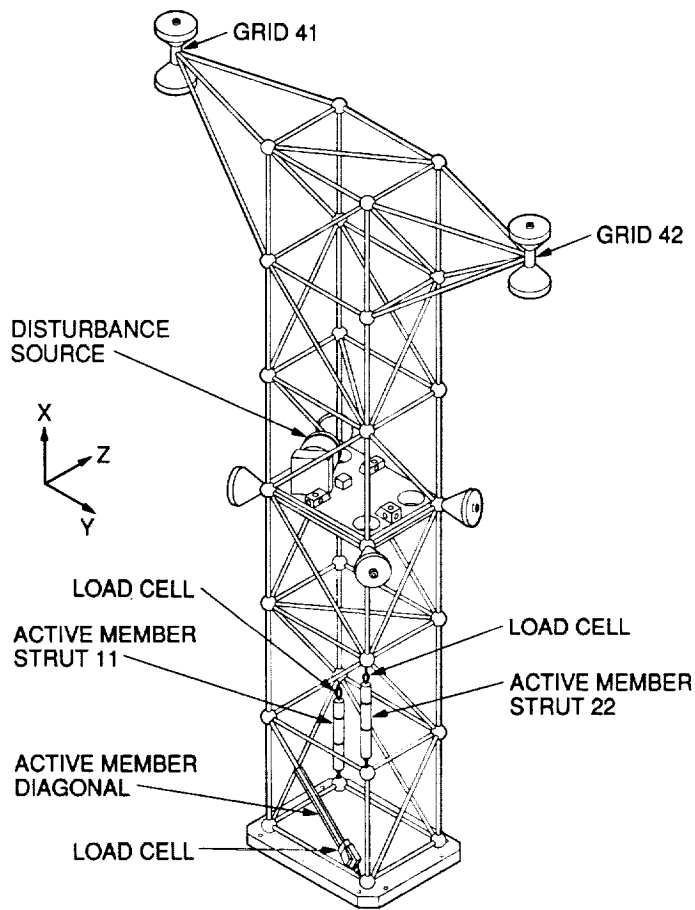
- Stiff Structural Members
- Low Current
- Operate Statically
- High Bandwidth
- Large Force
- Non-inertial Reacting
- Nanometer Precision

CHALLENGES

- Close Pole/Zero Pairs
- High Voltage
- Hysteresis
- Nonlinearity
- Small throw

DIAGRAM OF PRECISION TRUSS TEST BED

The subject of this research is the control of a truss structure called the Precision Truss. The Precision Truss has been designed to exhibit many of the salient features of structures that will form key components of next generation spacecraft. Specifically, the truss is stiff and statically indeterminate, the fundamental vibrational mode occurs below 10 Hz, the lower modes are closely spaced and coupled, and the structure possesses low inherent damping. Repeatable disturbances are injected into the truss by a small shaker mounted to a plate at the center bay of the truss.



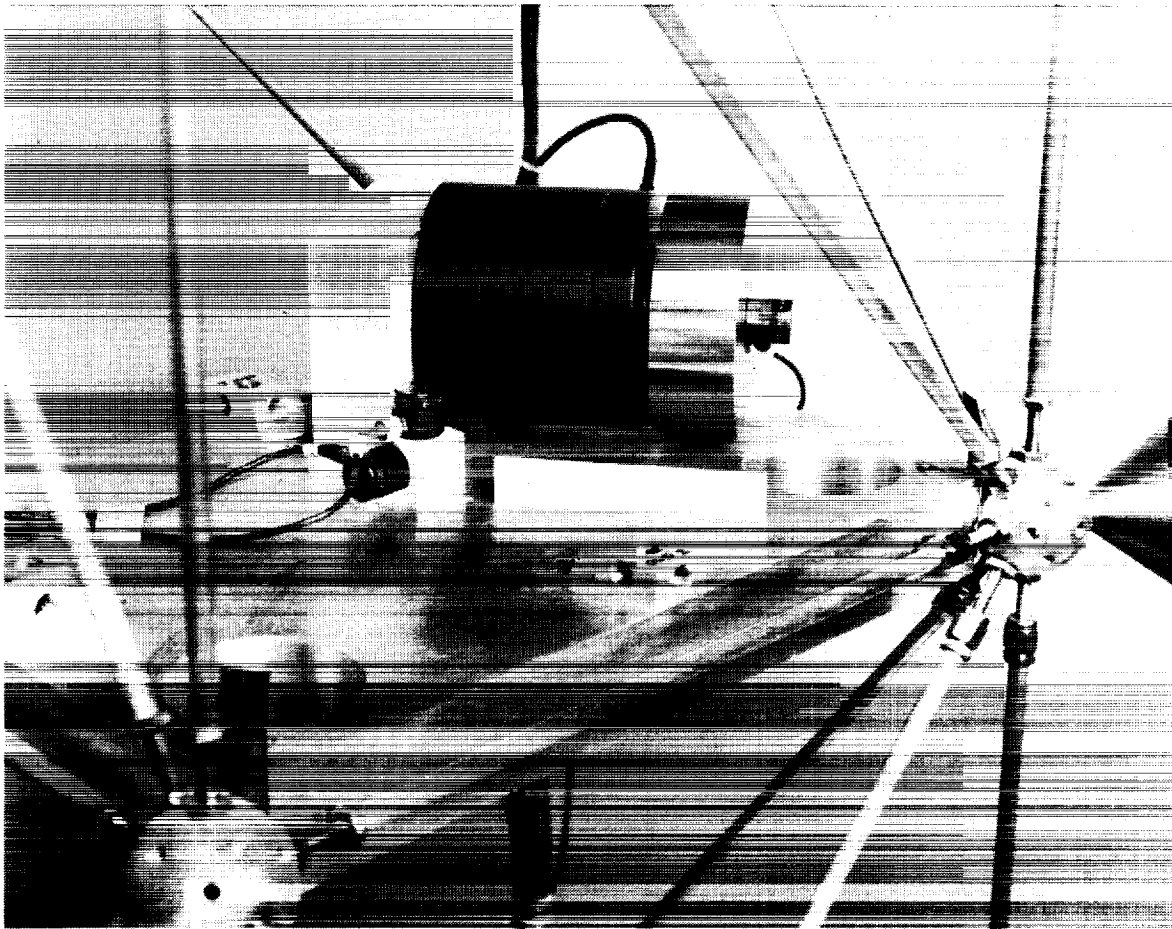
FREQUENCIES AND DAMPING COEFFICIENTS OF THE OPEN-LOOP STRUCTURE

The table lists the increase in passive damping of the structure with active-members compared to the structure without the active-members. The increase is due to the large level of hysteresis in the actuators. Shown are the first three modes--modes one and two are cantilever bending in two directions, the third mode is torsion. Higher modes appear at about 34 Hz. These data are from a modal survey of the Precision Truss using external excitation and active-member excitation¹¹.

| Mode | No Active-Members | | With Active-Members | |
|------|-------------------|-------------|---------------------|-------------|
| | f (Hz) | ζ (%) | f (Hz) | ζ (%) |
| 1 | 8.11 | 0.036 | 8.28 | 0.436 |
| 2 | 10.4 | 0.051 | 10.78 | 0.997 |
| 3 | 11.5 | 0.031 | 11.45 | 0.101 |

DISTURBANCE SOURCE

The center bay of the truss contains a rigid plate. Mounted to this plate is a 2.25 lbf electromagnetic shaker which is used to inject a repeatable disturbance into the structure. The shaker is oriented at an angle and offset from the center of symmetry so that it can excite not only bending modes in the y and z directions but also torsion along the vertical (x) axis. A 2 lb concentrated mass added to the armature of the shaker provides sufficient inertia for force to be applied to the truss at low frequency without requiring excessive armature motion.



ORIGINAL PAGE
BLACK AND WHITE PHOTOGRAPH

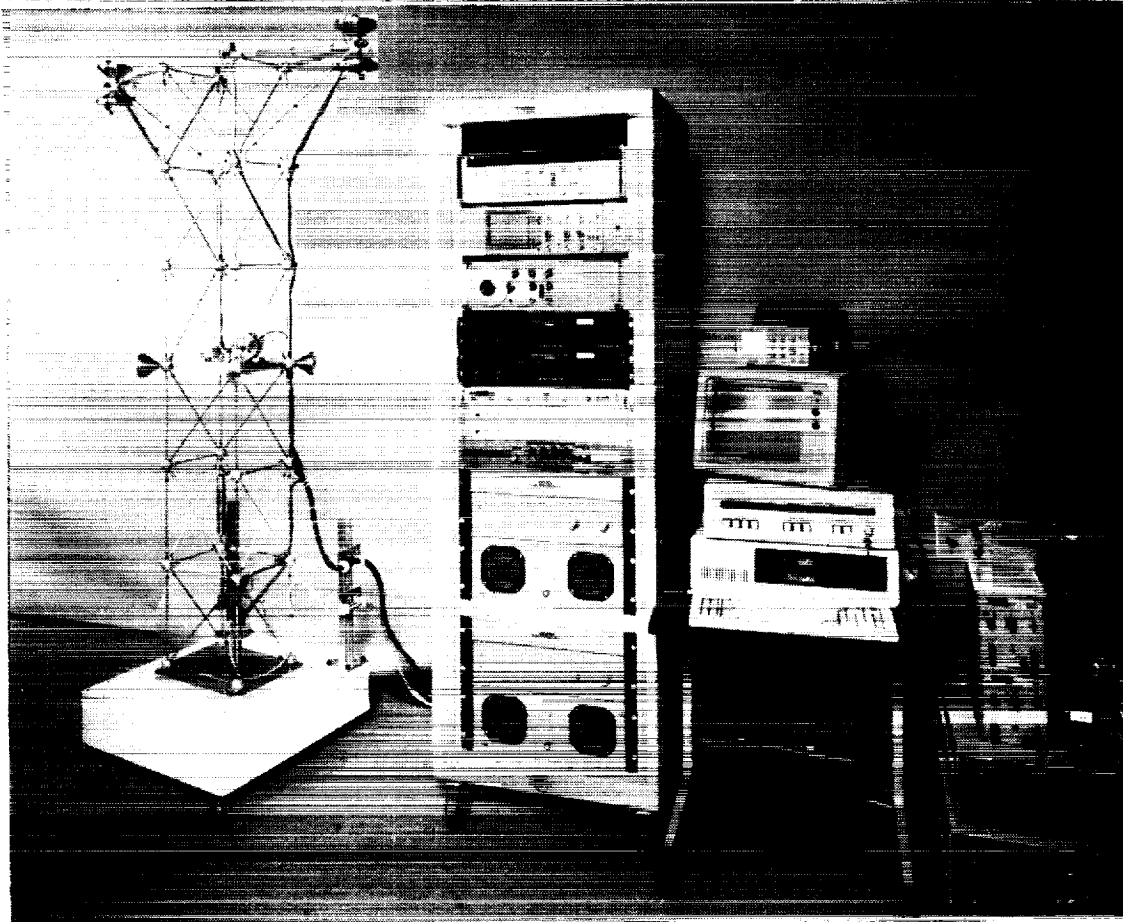
EXPERIMENTAL TEST SETUP FOR CLOSED-LOOP CONTROL

The photograph depicts the experimental setup used for closed-loop control tests. Apart from the active-members, which function as both sensors and actuators for the closed-loop control, the most significant hardware component is the Systolic Systems PC1000 digital array processor. The PC1000 digitizes analog signals at 2000 Hz, implements discrete state space control algorithms utilizing up to 32 states and 16 input signals, and commands up to 16 control outputs through a zero order hold. Variable amplifiers and an output smoothing filter are also used in the closed loop.

The ultimate objective of the phase 1 control experiments is to stabilize the motion of outrigger 41 subject to a narrowband disturbance at the midbay plate, while utilizing active-members in the lower three bays of the truss. The locations of the three active-members have been optimized for this control objective. The first controllers we have implemented are simple low order SISO* designs; more sophisticated control designs utilizing all three active-members are planned for the coming year. An attempt will be made to later extend the level of control to the submicron regime.

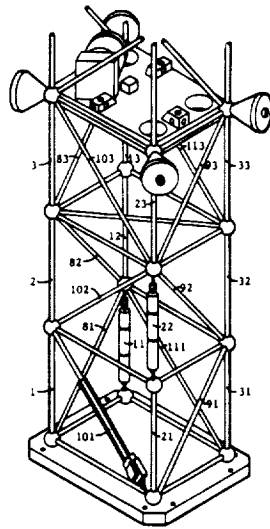
*single-input, single-output

ORIGINAL PAGE
BLACK AND WHITE PHOTOGRAPH



ACTUATOR PLACEMENT SELECTION

Three active-members were available for placement in the Precision Truss structure. The lower bays are an intuitive place to locate the active-members because most of the strain energy for the lower modes occurs near the cantilevered end. A methodology for selecting the optimal locations considers a stationary colored noise disturbance (20 Hz bandwidth) entering at the midbay plate. Performance was defined as $\gamma \|y\|_2 + \|u\|_2$, where y is measured at outrigger 41, u is control effort, and γ is a scaling parameter. For any set of locations, this leads to a well posed \mathcal{H}_2 -optimization problem¹². In order to reduce the number of possible locations to a more tractable set, a preliminary selection was performed by first solving the \mathcal{H}_2 -optimization problem assuming that an active-member could be placed in all possible locations simultaneously. From the solution to this optimization, the total energy in each control input was computed and ranked. The heuristic argument is that the active-member locations which perform the most work are superior locations for control. A subset of locations with the highest control input energy was selected for subsequent combinatorial optimization. The result of this process for the Precision Truss suggested that the optimal locations were two longerons in the first and second bays and one diagonal in the first bay.



Number Scheme for Longerons and Diagonals in Lower Three Bays

Control Effort for Actuators for Preselection of Candidate Locations

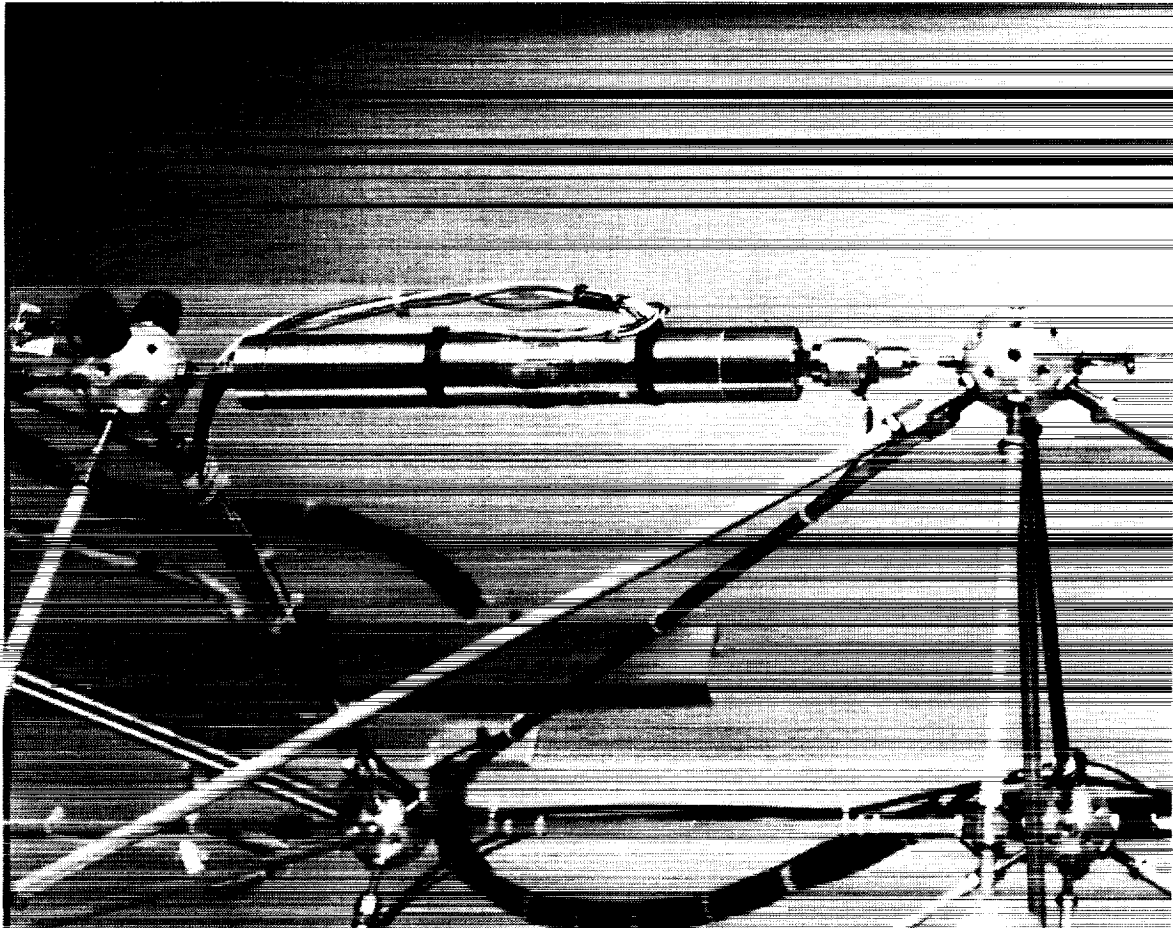
| Actuator # | Element # | $\ u\ _2$ |
|------------|-----------|-----------|
| 3 | 11 | 10.92815 |
| 6 | 21 | 8.47903 |
| 10 | 22 | 8.47496 |
| 2 | 101 | 7.22583 |
| 12 | 12 | 6.23132 |
| 20 | 13 | 6.22398 |
| 21 | 103 | 5.84743 |
| 15 | 82 | 5.79099 |
| 9 | 2 | 5.05582 |
| 18 | 23 | 4.15259 |
| 24 | 83 | 4.13487 |
| 13 | 42 | 3.79535 |
| 5 | 111 | 3.35653 |
| 4 | 81 | 3.27266 |
| 7 | 31 | 3.23416 |
| 8 | 91 | 3.07798 |
| 11 | 32 | 2.84030 |
| 23 | 113 | 2.62724 |
| 16 | 112 | 2.48088 |
| 17 | 3 | 2.31858 |
| 22 | 93 | 2.25864 |
| 1 | 1 | 2.17953 |
| 14 | 92 | 2.13915 |
| 19 | 33 | 1.77798 |

Ranking of Actuator Selection Pairs

| Element # | Cost | $\ u\ _2$ | $\ y\ _2$ | $\frac{\ y\ _2}{\ u\ _2}$ | $\frac{\ y\ _2}{\ y_{open}\ _2}$ |
|-------------|-------------|-------------|-------------|---------------------------|----------------------------------|
| 101, 11, 21 | 6.87284e+01 | 5.08403e+01 | 4.62478e-03 | 9.09668e-05 | 1.42634e-02 |
| 101, 11, 22 | 6.87336e+01 | 5.08466e+01 | 4.62487e-03 | 9.09573e-05 | 1.42637e-02 |
| 101, 11, 12 | 7.15809e+01 | 5.39124e+01 | 4.70879e-03 | 8.73416e-05 | 1.45226e-02 |
| 101, 11, 13 | 7.15896e+01 | 5.39231e+01 | 4.70890e-03 | 8.73263e-05 | 1.45229e-02 |
| 101, 21, 22 | 7.56169e+01 | 5.46423e+01 | 5.22699e-03 | 9.56584e-05 | 1.61207e-02 |
| 101, 21, 12 | 7.92828e+01 | 5.84258e+01 | 5.35928e-03 | 9.17280e-05 | 1.65287e-02 |
| 101, 21, 13 | 7.92953e+01 | 5.84392e+01 | 5.35967e-03 | 9.17136e-05 | 1.65300e-02 |
| 101, 22, 12 | 7.92965e+01 | 5.84367e+01 | 5.36012e-03 | 9.17252e-05 | 1.65313e-02 |
| 101, 22, 13 | 7.93090e+01 | 5.84501e+01 | 5.36051e-03 | 9.17108e-05 | 1.65325e-02 |
| 101, 12, 13 | 8.66331e+01 | 6.34581e+01 | 5.89776e-03 | 9.29395e-05 | 1.81895e-02 |
| 11, 21, 22 | 8.26441e+01 | 4.44797e+01 | 6.96534e-03 | 1.56596e-04 | 2.14821e-02 |
| 11, 21, 13 | 8.41313e+01 | 4.68191e+01 | 6.99002e-03 | 1.49298e-04 | 2.15582e-02 |
| 11, 21, 12 | 8.41299e+01 | 4.68096e+01 | 6.99050e-03 | 1.49339e-04 | 2.15596e-02 |
| 11, 22, 13 | 8.41427e+01 | 4.68172e+01 | 6.99153e-03 | 1.49337e-04 | 2.15628e-02 |
| 11, 22, 12 | 8.41414e+01 | 4.68077e+01 | 6.99201e-03 | 1.49377e-04 | 2.15643e-02 |
| 11, 12, 13 | 8.68547e+01 | 4.89402e+01 | 7.17537e-03 | 1.46615e-04 | 2.21298e-02 |
| 21, 22, 13 | 1.02464e+02 | 5.23094e+01 | 8.81057e-03 | 1.68432e-04 | 2.71730e-02 |
| 21, 22, 12 | 1.02488e+02 | 5.22436e+01 | 8.81723e-03 | 1.68772e-04 | 2.71935e-02 |
| 22, 12, 13 | 1.06296e+02 | 5.59834e+01 | 9.03585e-03 | 1.61402e-04 | 2.78678e-02 |
| 21, 12, 13 | 1.06314e+02 | 5.59464e+01 | 9.04031e-03 | 1.61589e-04 | 2.78815e-02 |

PIEZOELECTRIC ACTIVE MEMBERS

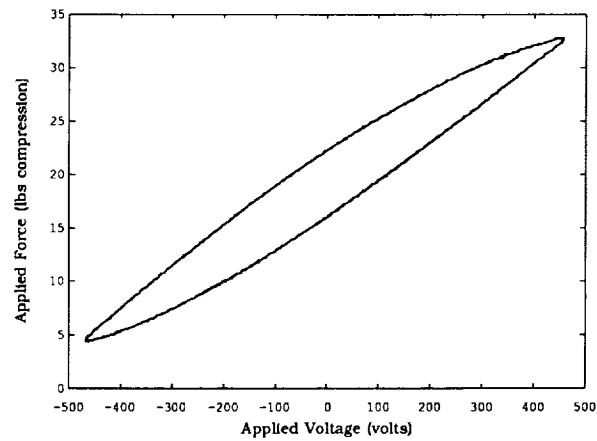
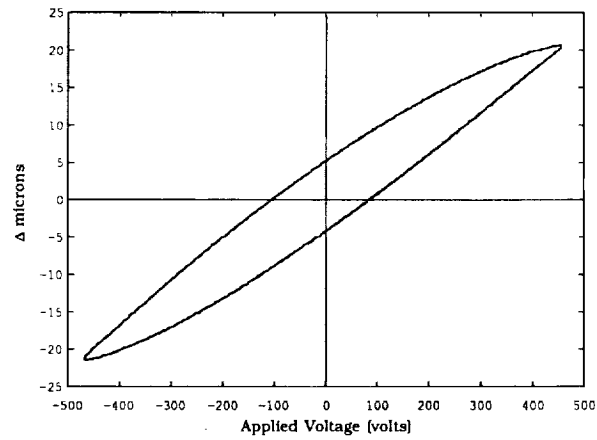
Two types of piezoelectric active-members are used in the truss. The first type is a low voltage piezoelectric actuator ordinarily used for fine positioning of optics. This device has a throw of 106 microns at 150 volts. The device has a relatively low stiffness of 23,300 lb/in which leads to a clamped force of 97 lb. The second type of active-member is a constant length strut (CLS) built to JPL specifications by Kaman Instrumentation Inc. This device makes use of a high voltage piezoelectric wafer stack in series with a stainless steel tube extension. The piezoelectric stack expands and contracts with applied voltage producing a relative motion between the two ends of the strut. A quartz reference rod (selected for low coefficient of thermal expansion) is attached rigidly to the moving end (armature) and extends down the length of the strut along the centerline. A differential eddy-current proximity sensor is built into the opposite end of the strut. This sensor measures the motion of a target disc attached to the reference rod, thereby measuring the change in the length of the strut. This sensor has a resolution of 1 nanometer.



ORIGINAL PAGE
BLACK AND WHITE PHOTOGRAPH

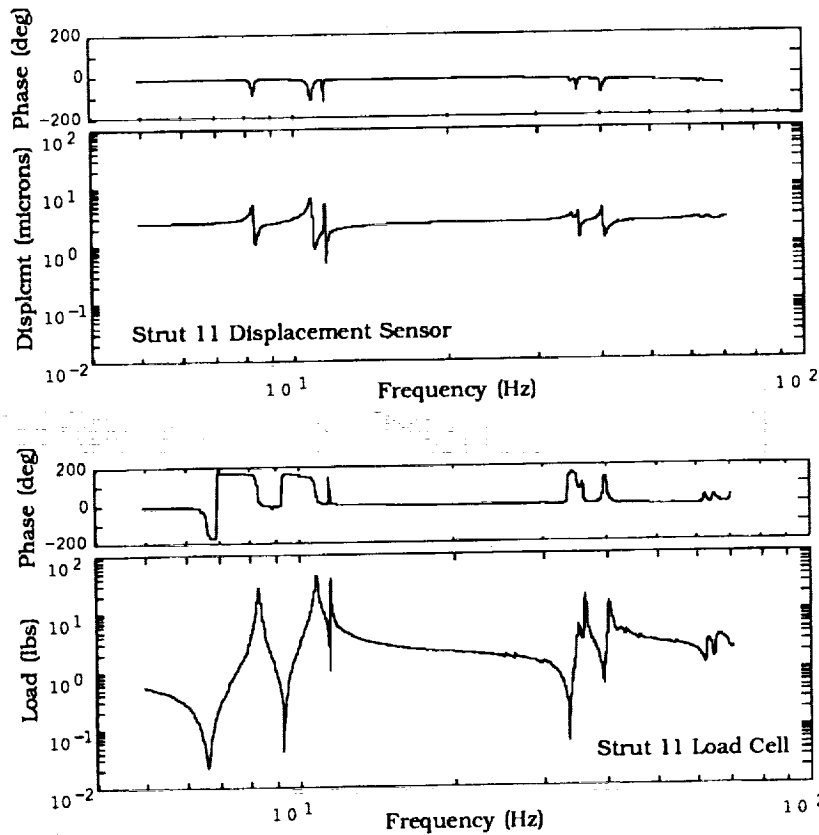
HYSTERESIS OF ACTIVE MEMBERS

Each active-member was tested in a calibration fixture. The Kaman CLS struts were found to exhibit approximately 20% hysteresis, due to the piezoelectric material used in the actuators.



OPEN-LOOP STRUCTURE--MEASURED DATA

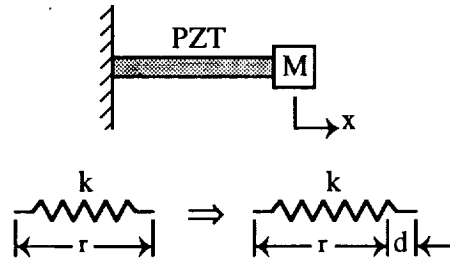
The active-member in the longeron of the first bay (strut 11) was selected as the sole actuator for the initial single-input-single-output control tests. For feedback measurements, it was convenient to use signals from the strut internal displacement sensors. Input-output transfer functions from strut 11 to the two internal displacements were measured using a stepped-sine test and are shown in the figure. Close pole-zero spacing is very pronounced for the collocated transfer function, due to a large feedthrough term corresponding to the residual flexibility of the structure at that actuator location. The feedthrough term was not present for the noncollocated displacement or for either load cell in series with the active-members.



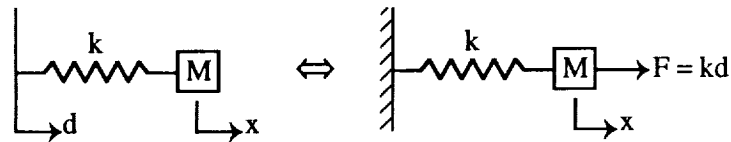
ACTIVE-MEMBER PHENOMENOLOGY

The observed close pole-zero spacing warranted further investigation into the behavior of the active-members. A model was developed for active-members in structures that makes use of externally applied forces at physical degrees of freedom. Were the active-member perfectly linear, it could be modelled as a structural element of length r and stiffness k which, if unconstrained, changes length by an amount d which is proportional to the electric field applied across the piezoelectric. As far as the dynamics of mass M are concerned, the variable length strut is equivalent to a moving boundary on a passive strut of stiffness k . The corresponding differential equation can be rearranged to produce the familiar equation of motion. Thus, the effect of the active-member on the dynamics of mass M can be modelled as an externally applied force kd applied to the interface point between the active-member and mass M .

- PHENOMENOLOGY



$$d = d_{33} E_f r \sim (100\mu\text{m})$$

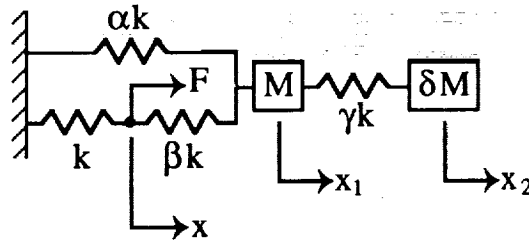


$$M\ddot{x} = k(d - x) \iff M\ddot{x} + kx = kd$$

$$kd_{\text{max}} = \text{clamped force} \sim (100\text{lb})$$

MODEL OF ACTIVE MEMBER IN STRUCTURE

An interesting phenomenon of close pole/zero pairs occurs when collocated displacement sensors are used in conjunction with active-members. Consider the simplified two degree of freedom model of the Precision Truss shown in the figure. A single active-member is represented as spring k , and the force F models the effect of the active-member on the structure. The collocated transfer function from d to x is computed. The parameter β represents the ratio of the input point stiffness to the active-member stiffness, and in general is less than unity. We see that as $\beta \rightarrow 0$ the poles and zeros quickly approach each other. Furthermore, as $s \rightarrow \infty$ the transfer function x/d does not approach zero, but rather approaches a constant value $1/(1+\beta)$. This represents a sizable feedthrough term.



$$kd = F, \omega = k/m, \epsilon = 1/\delta$$

$$\frac{x}{d} = \frac{s^4 + s^2(\alpha + \beta + \gamma + \gamma\epsilon)\omega^2 + (\alpha + \beta)\gamma\epsilon\omega^4}{[s^4 + s^2(\alpha + \beta + \gamma + \gamma\epsilon)\omega^2 + (\alpha + \beta)\gamma\epsilon\omega^4](1 + \beta) - (s^2 + \gamma\epsilon\omega^2)\omega^2\beta^2}$$

$$s \rightarrow 0 \quad \frac{x}{d} \rightarrow \frac{1}{1 + \frac{\alpha\beta}{\alpha + \beta}}$$

$$s \rightarrow \infty \quad \frac{x}{d} \rightarrow \frac{1}{1 + \beta}$$

$$\dot{\xi} = A\xi + Bd$$

$$\dot{x} = C\xi + Dd$$

POLE-ZERO SPACING OF MODEL

Solving for the system eigenvalues, the pole-zero spacing is found to be a function of the stiffness ratio β . The smaller the β (corresponding to a large actuator stiffness relative to the structure), the closer is the pole-zero spacing. Pole-zero spacing is small even for $\beta=1$.

$$a = (\alpha + \beta + \gamma + \gamma\epsilon), b = (\alpha + \beta)$$

for $\beta \ll 1$

zeros:

$$s^2 = -\frac{1}{2}a\omega^2 \pm \omega^2 \sqrt{\frac{1}{4}a^2 - b\gamma\epsilon}$$

poles:

$$s^2 = -\frac{1}{2}a\omega^2 \pm \omega^2 \sqrt{\frac{1}{4}a^2 - b\gamma\epsilon} \left[1 + \frac{\frac{1}{2}(\gamma\epsilon - \frac{1}{2}a)\beta^2\omega^2}{\frac{1}{4}a^2 - b\gamma\epsilon} \right] + \frac{1}{2}\beta^2\omega^2$$

EXAMPLE

$$k = \alpha = \beta = \delta = \gamma = 1$$

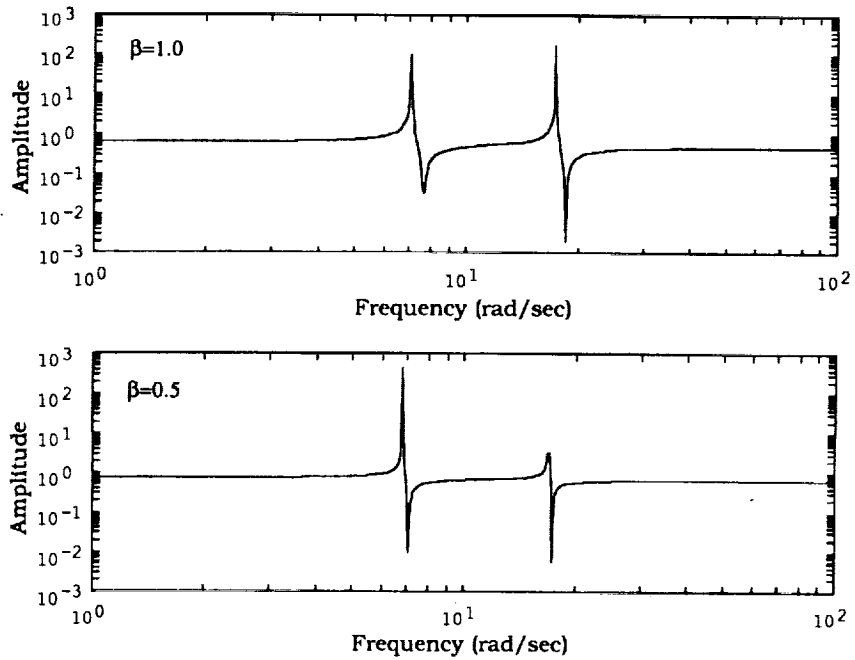
$$M = 0.01, \omega = 10$$

$$\text{poles} = \pm j 7.07, \quad \pm j 17.32$$

$$\text{zeros} = \pm j 7.68, \quad \pm j 18.50$$

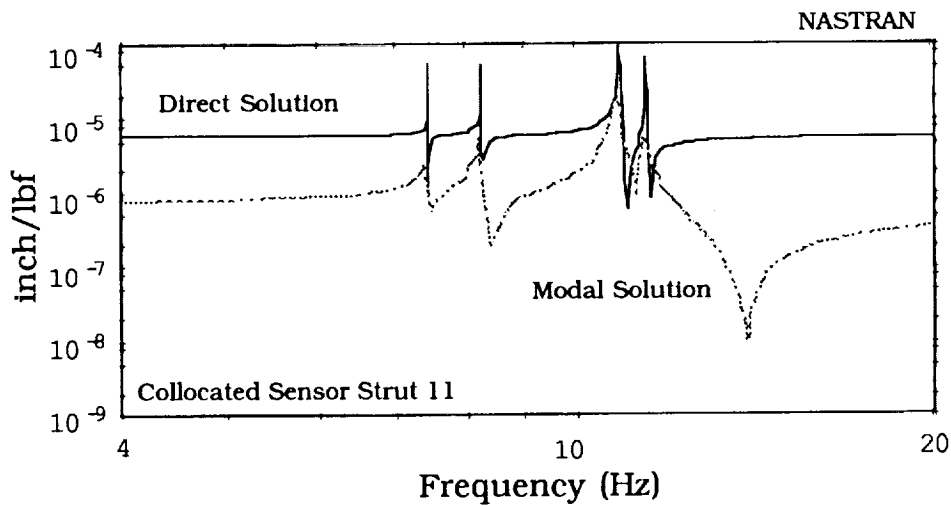
COLLOCATED TRANSFER FUNCTION OF MODEL

Collocated transfer functions of the active-member/structural model are shown for two values of the stiffness ratio β . The near pole-zero cancellation is readily seen. This phenomenon is not restricted to active-member applications but will occur any time a collocated measurement is made at a location where the structure is compliant with respect to the applied force.



COMPARISON OF NASTRAN DIRECT AND MODAL SOLUTIONS

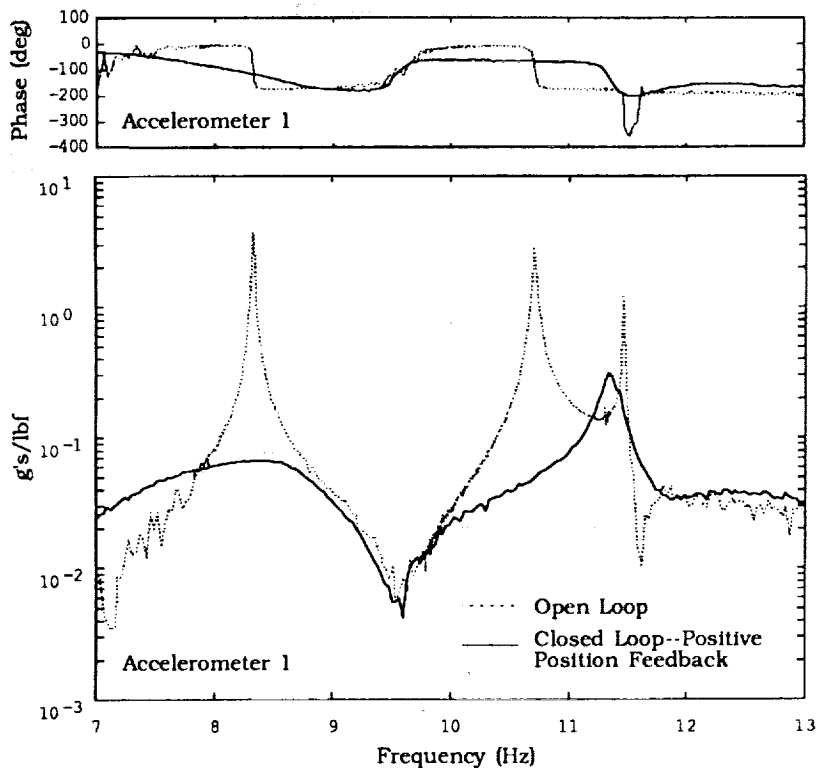
Care must be taken when obtaining the collocated transfer functions of the Precision Truss and other models via finite element models. The figure shows the collocated transfer function for strut 11 produced by NASTRAN. The solid curve is the result of a direct solution utilizing the system mass and stiffness matrices. The dashed curve is the same transfer function obtained by modal solution retaining the first 30 structural modes. There is substantial error in the modal solution both in the feedthrough term and in the transmission zero locations. Modal truncation, even as high as 30 modes, results in nearly complete loss of the residual flexibility between sensor and actuator.



CLOSED-LOOP CONTROL--POSITIVE POSITION FEEDBACK

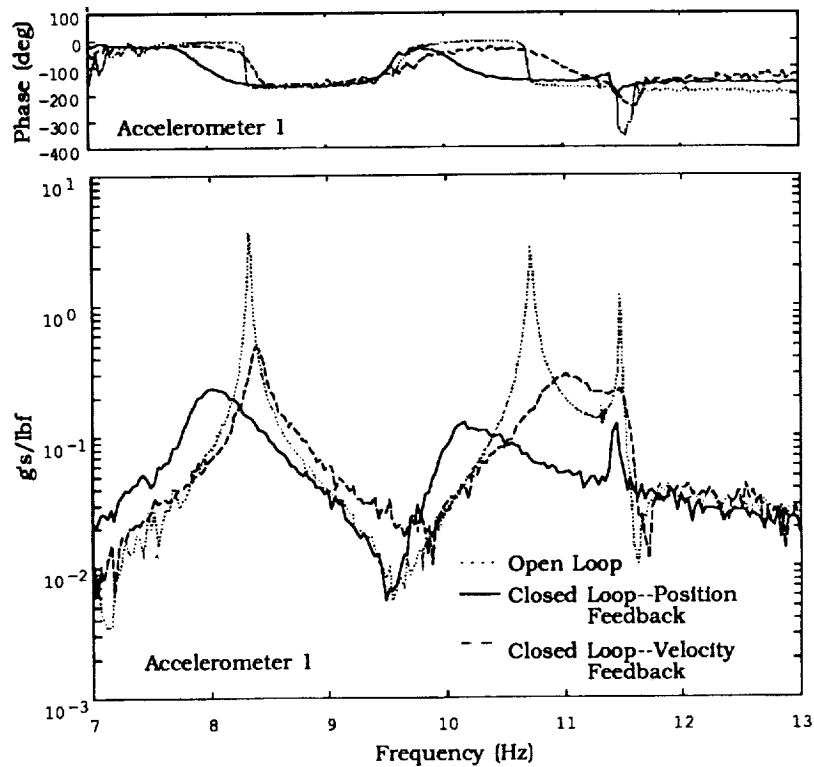
Four single-input-single-output controllers were designed for implementation using the digital array processor. Because the sampling rate of 2000 Hz was high relative to the control bandwidth, controllers were first designed in the continuous domain and were later discretized by a zero order hold approximation. Active-member 11 in the longeron of the first bay was chosen as the sole actuator for this study. The collocated and noncollocated displacement sensors in the longerons were selected as feedback measurements; accelerometer measurements at the outrigger provide a reference point for controller performance. Controllers were designed using Bode and root locus analysis.

The figure depicts a measured stepped-sine transfer function between the shaker disturbance and an accelerometer on the outrigger station 41 for both the open and closed loop cases. The positive position feedback design¹³ trades stiffness for damping and reduces the first mode amplitude by 35 dB. The third (torsional) mode displays some attenuation but is otherwise barely observable or controllable from longeron 11.



CLOSED-LOOP CONTROL--OUTPUT AND VELOCITY FEEDBACK

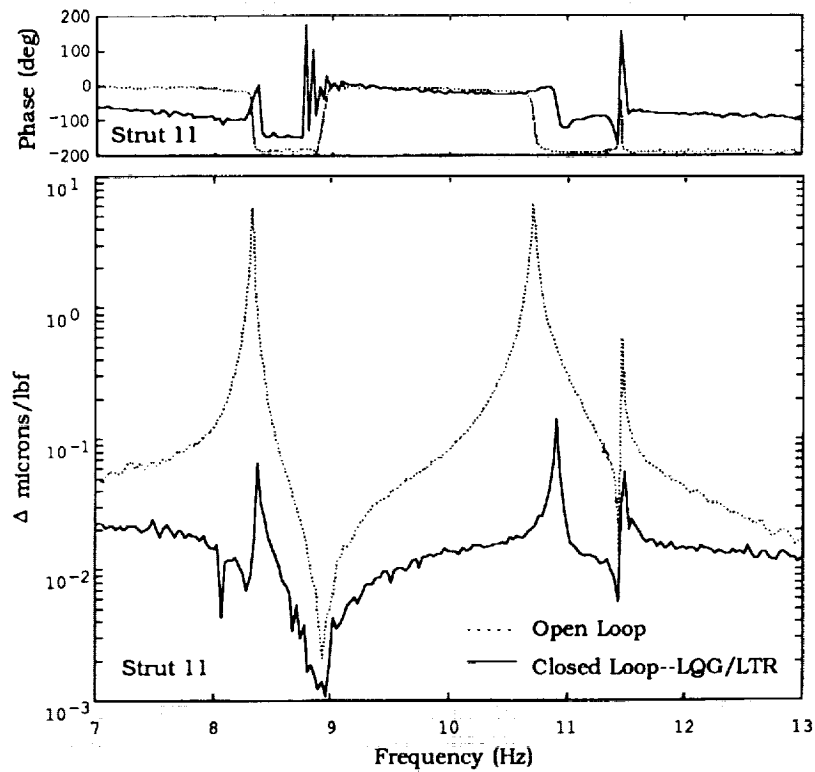
Output and velocity feedback designs were also implemented using the noncollocated internal displacement sensor from strut 22. Positive output feedback had the effect of softening the structure. Velocity feedback was implemented digitally by a second-order compensator with a 30 Hz rolloff. Spillover instability in the high modes limited the performance of each of these designs.



CLOSED-LOOP CONTROL--LQG/LTR

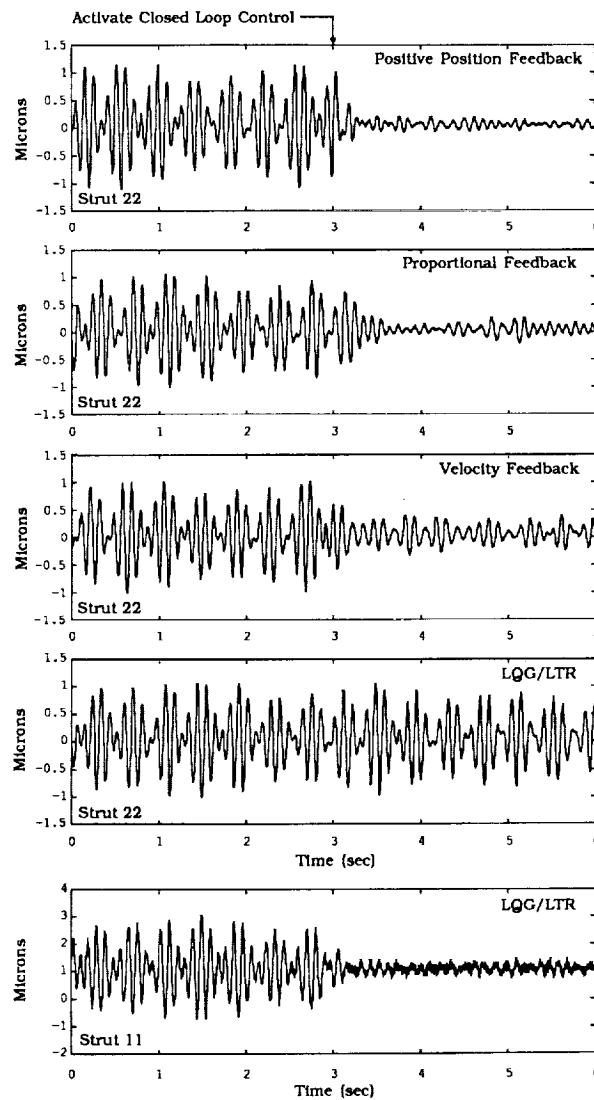
A sixth-order LQG/LTR* controller was implemented for the collocated internal displacement at strut 11. The figure shows the closed-loop transfer function at the design point, and demonstrates that while significant attenuation is achieved at this point, system damping is essentially unchanged. The resonances in the LQG/LTR closed-loop frequency response are due to the inaccuracies in a preliminary disturbance model used in the control design.

*linear quadratic Gaussian/loop transfer recovery



CLOSED-LOOP RESPONSE--NARROWBAND EXCITATION

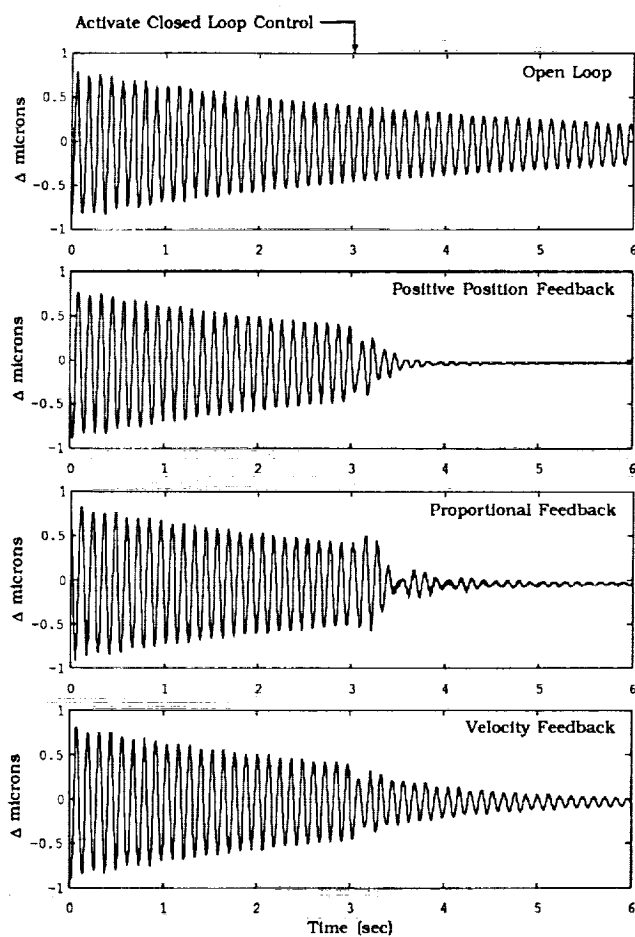
A second set of performance measurements was obtained by injecting a 5 to 15 Hz narrowband random excitation, using the shaker on the midbay plate, and observing the open and closed-loop steady-state response. The time histories are plotted in the figure for the response of the strut 22 internal sensor, the SISO design point. The beating pattern in the open-loop time histories is the result of the close coupling between the second (bending) and third (torsional) modes. The dramatic difference between LQG/LTR controller performance at strut 22 and the design point 11 further illuminates the localized nature of this controller.



FREE DECAY OF FIRST MODE

The third measurement of performance involves turning on the controllers midway through the free decay of the first (bending) mode. Positive Position Feedback* provides the best performance by increasing the damping from the open loop value of 0.436% to an estimated 8%. The PPF design was the most stable of the four designs implemented; the three others tended to drive some higher mode unstable at high loop gain. At high gain the PPF design leads to a static instability which results in saturation of the actuator. This type of instability is relatively benign compared to the potentially destructive effects of a dynamic instability.

*ppf



CONCLUSIONS

The objectives of this study were to close a digital control loop around a piezoelectric active-member in a representative truss structure and achieve improved performance over the open loop structure. These objectives have been achieved. A method for optimal actuator placement was implemented that makes use of a heuristic preselection process that greatly reduces the combinatorial possibilities of candidate actuator locations. The single-input-single-output control designs implemented were relatively simple and no attempt was made to extract optimal performance from these systems. Nevertheless, the response of the first two bending modes of the structure was attenuated by more than 35 dB and damping was increased by a factor of 20 to eight percent.

We have observed and explained analytically that high feedthrough terms are likely to exist in collocated measurements of active members, terms which correspond to the quasi-static "residual flexibility" of higher modes. The feedthrough terms result in close pole-zero pairs which complicate the control design.

Future research will explore the use of more sophisticated multivariable control methodologies for improved performance.

REFERENCES

1. Laskin, R. A., "A Spaceborn Imaging Interferometer - The JPL CSI Mission Focus," presented at the Third NASA/DOD Controls Structures Interaction Technology Conference, San Diego, CA, January 29 -- February 2, 1989.
2. Dailey, L. R., and Lukich, M., "Recent Results in Identification and Control of Flexible Truss Structure," *Proceedings of the American Control Conference*, Atlanta GA, June 1988. pp. 1468--1473.
3. Balas, G. J., and Doyle, J. C., "On the Caltech Experimental Large Space Structure on and Control of Flexible Truss Structure," *Proceedings of the American Control Conference*, Atlanta GA, June 1988. pp. 1701--1702.
4. Natori, M., Motohashi, S., Takahara, K., and Kuwao, F., "Vibration Control of Truss Beam Structures Using Axial Force Actuators," *Proceedings of the 29th AIAA SDM Conference*, Williamsburg, VA, April 18 -- 20, 1988. pp. 491--499.
5. Crawley, E. F., and de Luis, J., "Use of Piezo-Ceramics as Distributed Actuators in Large Space Structures," *Proceedings of the 26th AIAA SDM Conference*, 1985.
6. Hanagud, S., Obal, M. W., and Meyyappa, M., "Electronic Damping Techniques and Active Vibration Control," *Proceedings of the 26th AIAA SDM Conference*, 1985.
7. Bailey, T. L., and Hubbard, J. E., "Distributed Piezoelectric Polymer Active Vibration Control of a Cantilever Beam," *Journal of Guidance, Control, and Dynamics*, Vol. 8, Sept.--Oct. 1985, pp. 605--611.
8. Fanson, J. L., and Chen J-C., "Vibration Suppression by Stiffness Control," *Proceedings of the Workshop on Structural Dynamics and Control Interaction of Flexible Structures*, Marshall Space Flight Center, April 22-24, 1986.

9. Hagood, N. W., and Crawley, E. F., "Development and Experimental Verification of Damping Enhancement Methodologies for Space Structures," MIT SSL#18-88, September, 1988.
10. Chen, G-S, Lurie, B. J., and Wada, B. K., "Experimental Studies of Adaptive Structures for Precision Performance," AIAA paper 89-1327, 1989.
11. Chen, J-C., and Fanson, J. L., "System Identification Test Using Active-Members," AIAA paper 89-1290, 1989.
12. Doyle, J. C., Glover, K., Khargonekar, P., and Francis B. A., "State-Space Solutions to Standard H_2 and H_∞ Control Problems," 1988 American Control Conference, Atlanta, GA.
13. Fanson, J. L., and Caughey, T. K., "Positive Position Feedback Control for Large Space Structures," *Proceedings of the 28th AIAA Dynamics Specialists Conference*, Monterey, CA, April 9--10, 1987. pp. 588--598.